



# Mechanism of Noise Generation on Outer Rotor Motor

Kazumasa IKEDA<sup>1</sup>; Junichi SEMURA<sup>2</sup>; Tsukasa OHZAWA<sup>3</sup>

<sup>1,2,3</sup> DENSO CORPORATION, Japan

## ABSTRACT

A rotor and a stator of an outer rotor motor often resonate with electromagnetic force working between them. Sometimes resonating rotor and stator cause irritating magnetic noise. When they make noises with their resonance, noise from the stator shows its resonance frequency. However, noise from the rotor shows different frequency from its resonance frequency. To clarify the mechanism of the phenomenon, surface vibration of the rotor during rotation was measured by using cylindrical microphone array that covered the entire rotor and was calculated by using advanced non-stationary conformal mapping technology by Equivalent Source Method (ESM) approach. As a result, it was found that the rotor is resonating with rotation and the amplitude of air vibration is modulated on the surface of the rotor.

Keywords: Noise, Resonance, Outer rotor motor

## 1. INTRODUCTION

The HVAC (Heating, Ventilation, and Air Conditioning) system is used for providing comfortable environment in vehicle cabin and consists of a main unit and a blower unit. In the blower unit, a fan directly connected to a motor generates air flow.

Referring to noise around blower unit, we are able to divide the noise into aerodynamic noise and electromagnetic noise. The aerodynamic noise of the blower fan is generated with air flow in wide range of frequency and the electromagnetic noise of the blower motor often appears as a peak at a certain frequency as shown in Figure 1.

In this study, we focused on the electromagnetic noise measured around 2000 Hz. The electric motor consists of a stator and a rotor and electromagnetic force working between them excites resonance of them<sup>(1-3)</sup>. The noise is caused by the resonance, however, it was confirmed that frequency of the electromagnetic noise is different from the resonance frequency of the rotor. In this paper, we clarified the mechanism that explains noise generation from the rotor comparing with one of the stator.

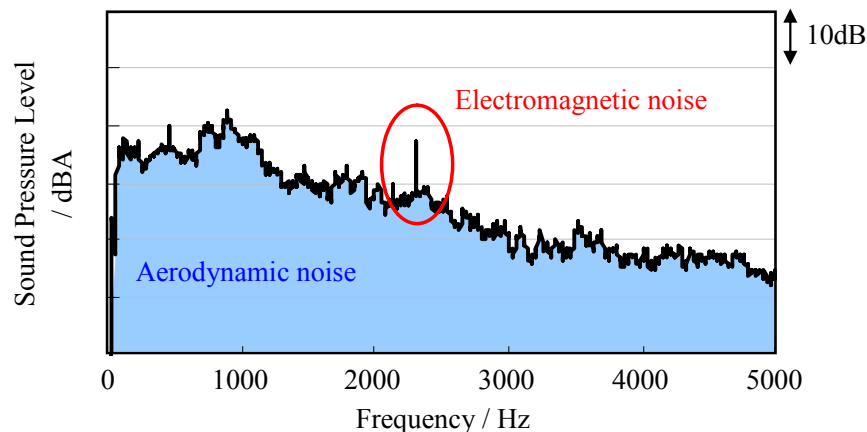


Figure 1 – Aerodynamic noise and electromagnetic noise of blower unit

<sup>1</sup> [kazumasa\\_ikeda@denso.co.jp](mailto:kazumasa_ikeda@denso.co.jp)

<sup>2</sup> [junich\\_semura@denso.co.jp](mailto:junich_semura@denso.co.jp)

<sup>3</sup> [tsukasa\\_ohzawa@denso.co.jp](mailto:tsukasa_ohzawa@denso.co.jp)

## 2. MEASUREMENT SYSTEM

### 2.1 Motor Sample

In this study, electromagnetic noise from two types of motor are measured and compared. Generally, an inner rotor motor has a rotor inside of a stator and an outer rotor motor has a rotor outside of a stator. We used the inner rotor motor for measuring the noise from the stator and the outer rotor motor for measuring the noise from the rotor.

#### 2.1.1 Inner Rotor Motor

The inner rotor motor used in this study is shown in Figure 2. Resonance characteristics of the stator are obtained by impact testing as shown in Figure 3. Figure 3(a) shows inertance and it is confirmed that the resonance frequency is 1926 Hz. Figure 3(b) shows the resonance mode viewed from axial direction. It is clarified that ellipsoidal shape is excited.

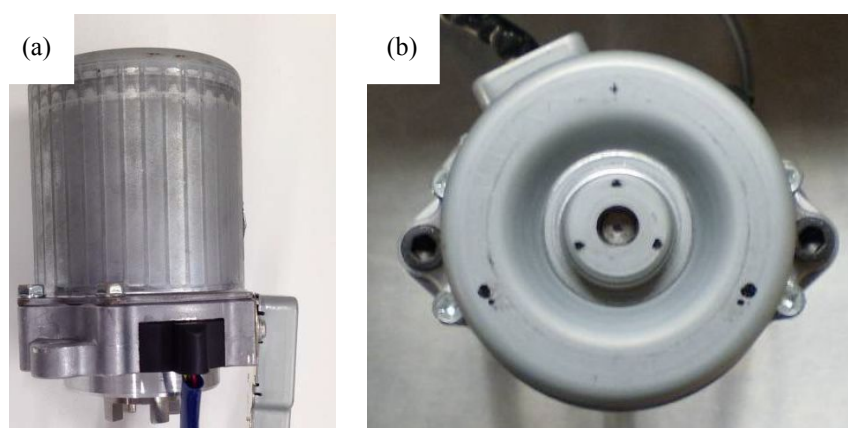


Figure 2 – Inner rotor motor  
(a)Side view (b)Plan view

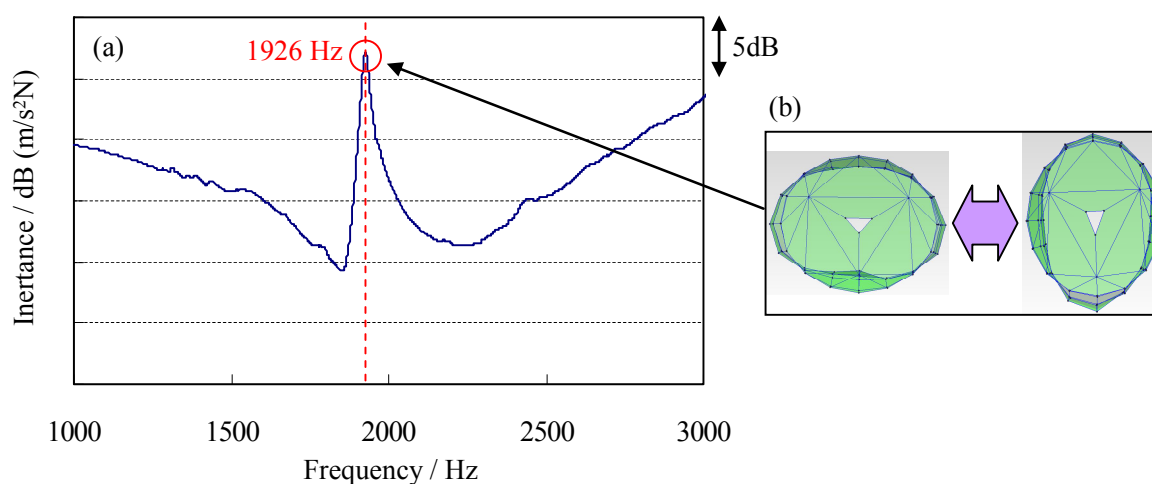


Figure 3 – Resonance characteristics of inner rotor motor  
(a)Inertance (b)Resonance mode

#### 2.1.2 Outer Rotor Motor

The outer rotor motor used in this study is shown in Figure 4. Resonance characteristics of the rotor are obtained by impact testing as shown in Figure 5. Figure 5(a) shows inertance and it is confirmed that the resonance frequency is 2226 Hz. Figure 5(b) shows the resonance mode viewed from axial direction. It is clarified that ellipsoidal shape is excited.

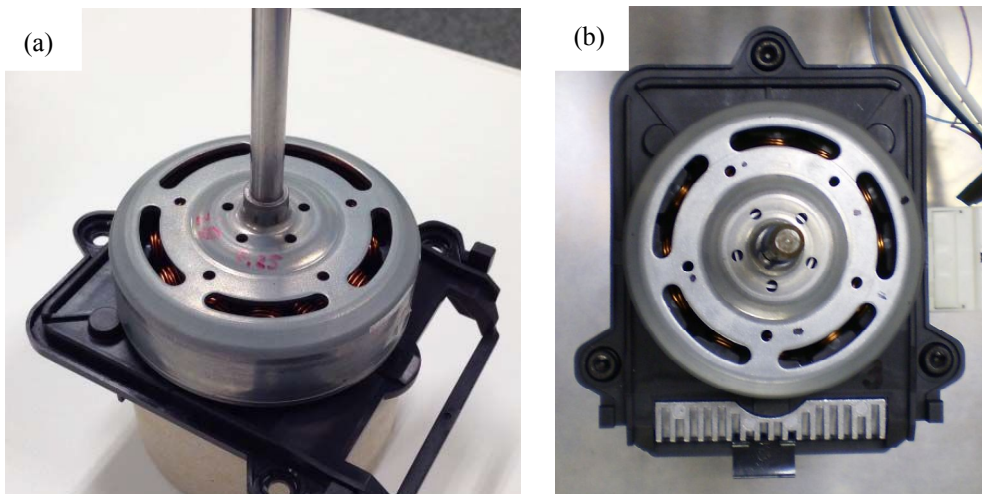


Figure 4 – Outer rotor motor  
(a)Perspective view (b)Plan view

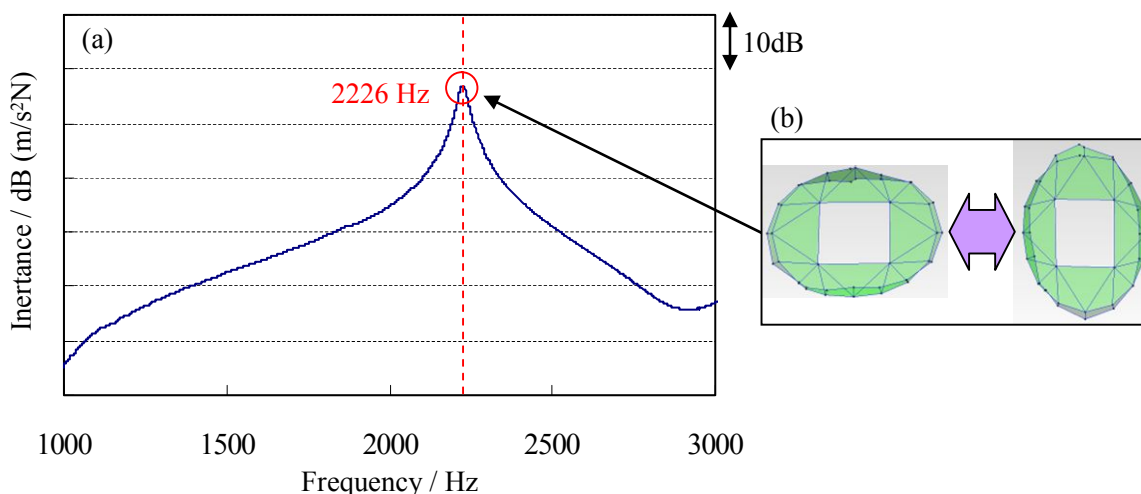


Figure 5 – Resonance characteristics of outer rotor motor  
(a)Inertance (b)Resonance mode

## 2.2 Non-stationary Conformal Mapping System

There are three typical methods to measure vibration of objects. One is the method using accelerometers that should be connected to devices with cable so they can not be used for rotating rotors. Another is the method using Laser Doppler Velocimeter (LDV). Studies have been reported that surface vibration of rotating disks was measured using LDV<sup>(4)</sup>. Although LDV can be used for a plane surface like disks, we could not measure vibration of the rotors that have curved surface because of lack of sensitivity.

Because it is difficult to directly measure vibration of objects, we focused on the other method; non-stationary conformal mapping technology that calculates air vibration nearby objects by measuring sound pressure. Moreover, in order to apply this technology to curved objects, we used a device introduced Equivalent Source Method (ESM) in which point sound sources are defined and vibration on them is calculated using sound pressure on measurement surface<sup>(5)</sup>. Figure 6 shows cylindrical microphone arrays covering objects. The array for inner rotor motor has 15 microphone holders toward circumferential direction and 4 toward axial direction so that 60 microphones can be totally activated simultaneously. The array for outer rotor motor has 12 microphone holders toward circumferential direction, 3 toward axial direction and 12 around the top of rotor so that 48 microphones can be totally activated simultaneously. In the case that all microphone holders are

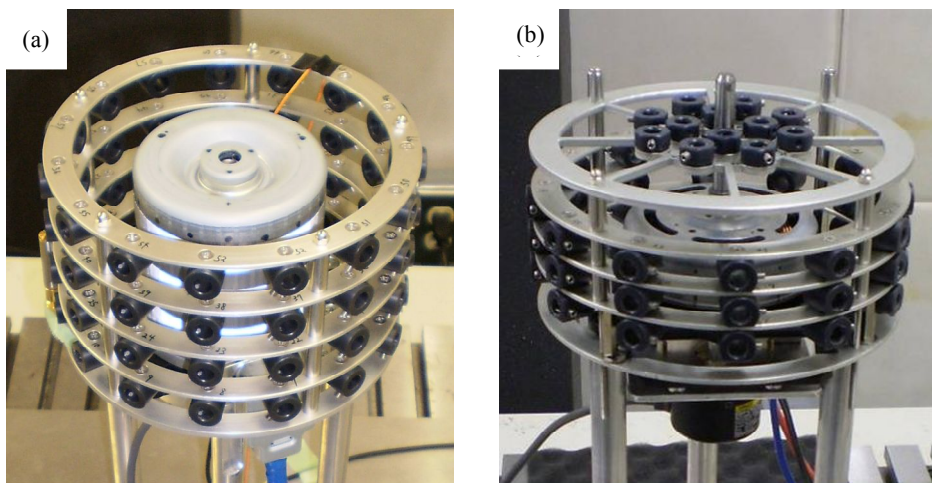


Figure 6 – Cylindrical microphone arrays  
 (a)For inner rotor motor (b)For outer rotor motor

filled, the arrays are able to cover frequency range of 100 to 6400 Hz according to distances among microphones and objects.

After calculation of vibration from sound pressure, 3D models of objects were used to display results. In this paper, the models were simplified and meshed as shown in Figure 7.

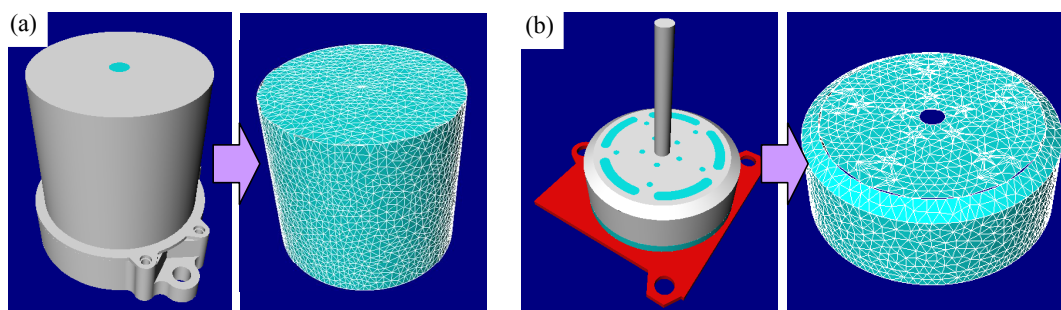


Figure 7 – Meshed models  
 (a)For inner rotor motor (b)For outer rotor motor

**2.3 Measurement Conditions**

First, a microphone was set nearby the side of objects and electromagnetic noise was measured. Then, the maximum sound pressure and the rotational speed when the sound pressure is the maximum were recorded. After that, vibration displacements of objects were calculated using the non-stationary conformal mapping system. The arrays with microphones are shown in Figure 8.

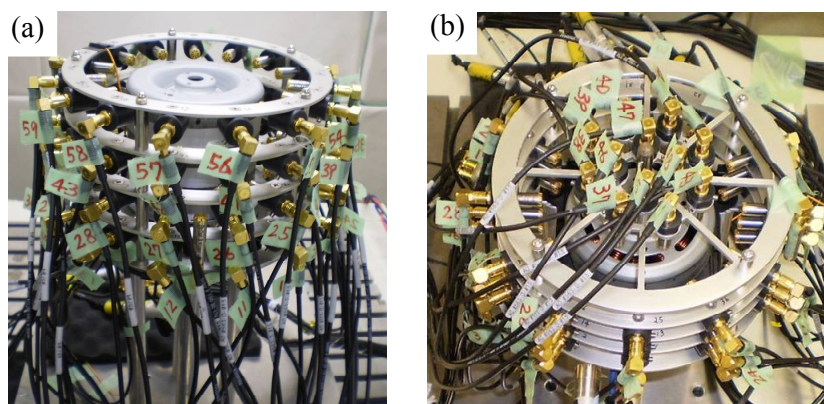


Figure 8 – Microphone-placed arrays  
 (a)For inner rotor motor (b)For outer rotor motor

### 3. MEASUREMENT

#### 3.1 Results of Non-Stationary Conformal Mapping for Inner Rotor Motor

The electromagnetic noise from the inner rotor motor was measured and showed maximum level when the rotational speed was 1650 rpm. The frequency characteristics are shown in Figure 9. The electromagnetic noise was maximized around 1926 Hz that is resonance frequency of the stator.

At the rotational speed 1650 rpm, vibration displacements on surface of the stator were measured at 1926 Hz using the non-stationary conformal mapping system. Figure 10 shows results at fixed intervals where  $T$  is defined as a cycle of vibration on any point of surface of the stator. In this figure, warm colors like yellow show positive displacement that means expansion toward outside of the stator and cool colors like blue show negative displacement that means contraction toward inside of the stator. Therefore, it is confirmed that the stator is resonating in ellipsoidal mode shown in Figure 3(b) with stationary wave.

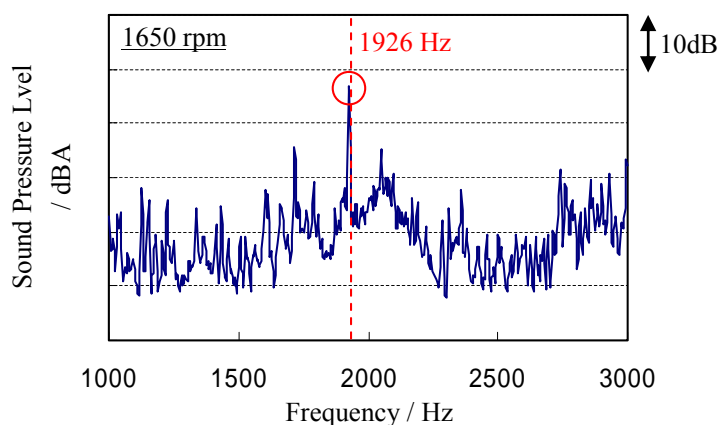


Figure 9 – Sound pressure level of inner rotor motor at 1650 rpm

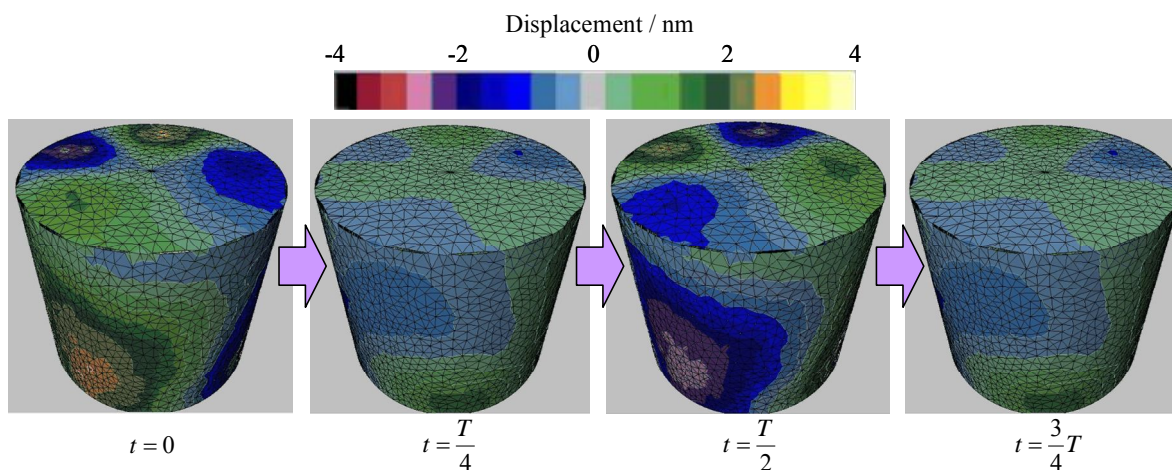


Figure 10 – Vibration displacements on surface of the stator at 1926 Hz

#### 3.2 Results of Non-Stationary Conformal Mapping for Outer Rotor Motor

##### 3.2.1 Entire Frequency Range

The electromagnetic noise from the outer rotor motor was measured and showed maximum level when the rotational speed was 2783 rpm. The characteristic of frequency and sound pressure level is shown in Figure 11. Noise shows two peaks sandwiching 2226 Hz that is resonance frequency of the rotor.

At the rotational speed 2783 rpm, vibration displacements on surface of the rotor were measured at the entire frequency range using the non-stationary conformal mapping system. Figure 12 shows results at a certain interval. Therefore, it is confirmed that the rotor is resonating in ellipsoidal mode shown in Figure 5(b) with moving stationary wave toward counterclockwise direction shown like black arrow in the figure.

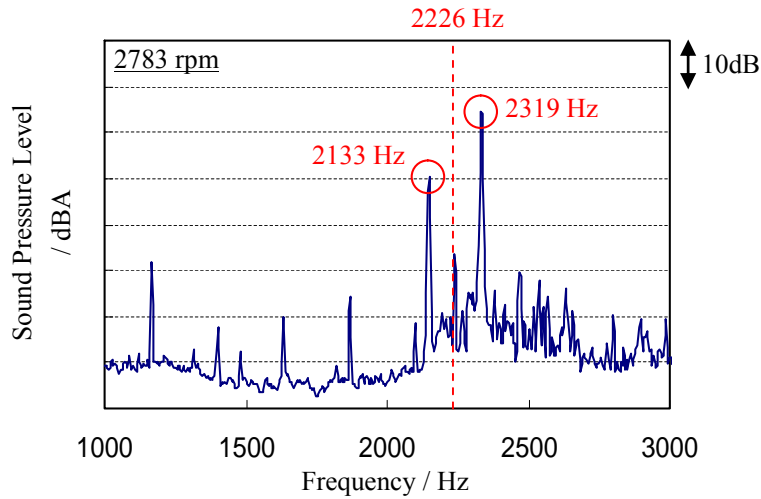


Figure 11 – Sound pressure level of outer rotor motor at 2783 rpm

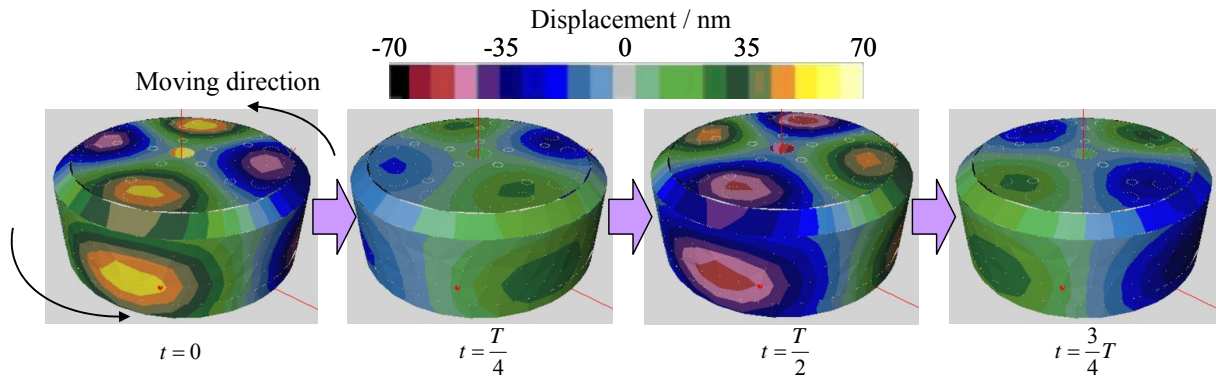


Figure 12 – Vibration displacements on surface of the rotor in the entire frequency range

### 3.2.2 The Peak at 2133 Hz

In order to analyze the peaks of the noise respectively, frequency range is adjusted to each peak. Figure 13 shows vibration displacements on surface of the rotor at 2133 Hz. It is found that the rotor is vibrating with clockwise polarized wave shown like black arrow in the figure.

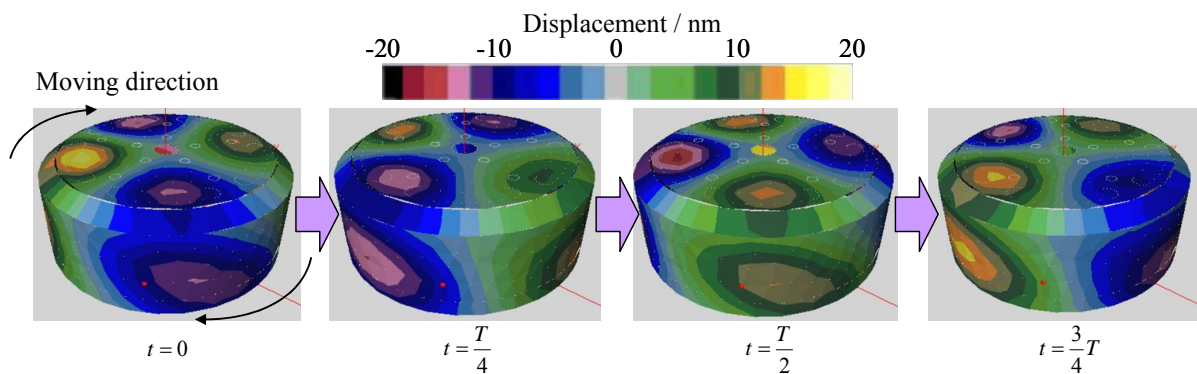


Figure 13 – Vibration displacements on surface of the rotor at 2133 Hz

### 3.2.3 The Peak at 2319 Hz

Figure 14 shows vibration displacements on surface of the rotor at 2319 Hz. It is found that the rotor is vibrating with counterclockwise polarized wave shown like black arrow in the figure.

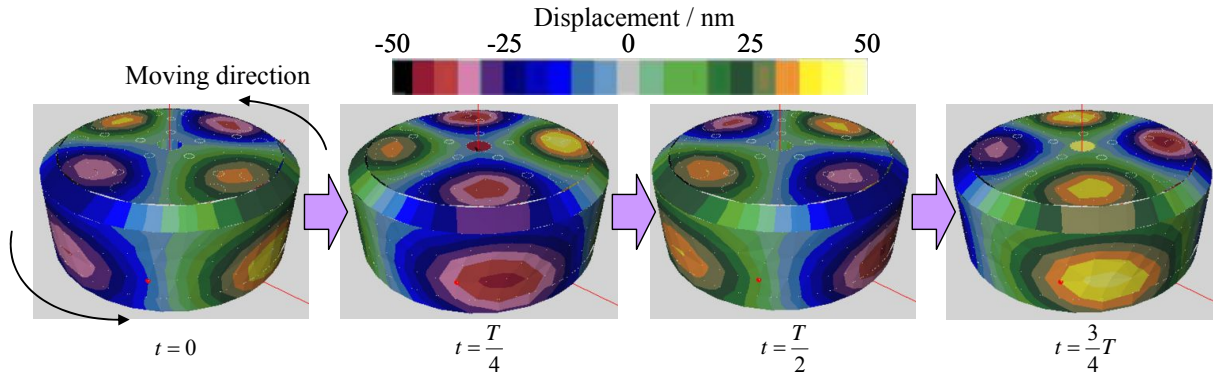


Figure 14 – Vibration displacements on surface of the rotor at 2319 Hz

#### 4. THEORETICAL CONSIDERATION

##### 4.1 Vibration of Stator

Assuming that cylindrical body shows ellipsoidal mode with stationary wave at its resonance frequency  $f_c$  described in Figure 15, we can express vibration displacements on surface of the body as following equation (1).

$$U(\theta, t) = U_0 e^{i2\theta} \frac{e^{i2\pi f_c t} + e^{-i2\pi f_c t}}{2} \tag{1}$$

Where  $U_0$  means maximum displacement and  $\theta$  means spatial phase.

This equation agrees with the results of the Figure 10 that shows stationary wave at the resonance frequency  $f_c = 1926$  Hz. Focusing on components of the equation, we are able to regard the stationary wave as the sum of a clockwise polarized wave and a counterclockwise polarized wave as following equation (1)' and shown in Figure 16.

$$U(\theta, t) = \frac{U_0}{2} e^{i(2\theta+2\pi f_c t)} + \frac{U_0}{2} e^{i(2\theta-2\pi f_c t)} = U_{CW}(\theta, t) + U_{CCW}(\theta, t) \tag{1}'$$

The two polarized waves fluctuate at the resonance frequency  $f_c$ .

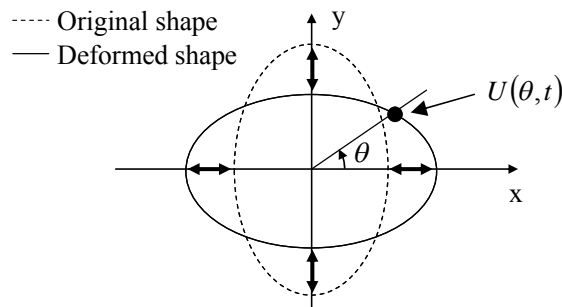


Figure 15 – vibration displacements on the surface of cylindrical body

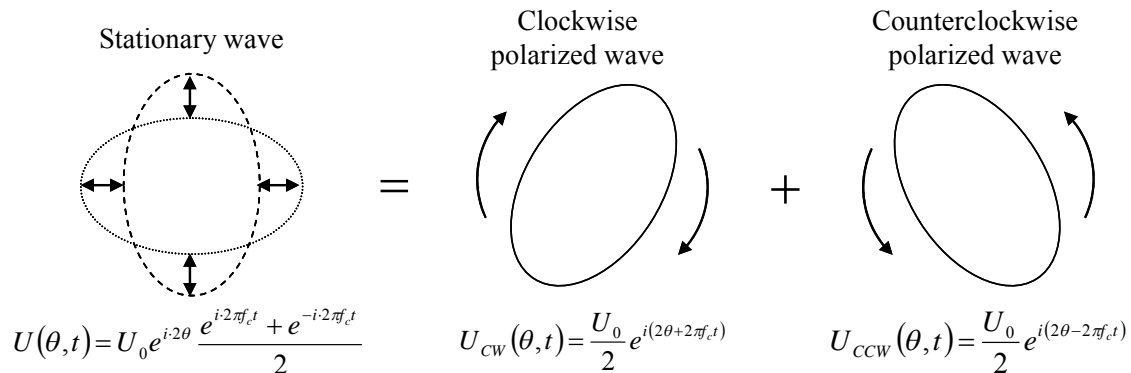


Figure 16 – Division of stationary wave into two polarized waves

## 4.2 Vibration of Rotor

Assuming that the mode described in the equation (1) is moving with the rotational speed  $\alpha_0$  [rps], we can express vibration displacements on surface of the body as following equation (2) on fixed coordinates system.

$$U(\theta, t) = U_0 e^{i2(\theta - 2\pi\alpha_0 t)} \frac{e^{i2\pi f_c t} + e^{-i2\pi f_c t}}{2} = U_0 e^{i2\theta} \frac{e^{i2\pi(f_c - 2\alpha_0)t} + e^{-i2\pi(f_c + 2\alpha_0)t}}{2} \quad (2)$$

The vibration displacements can be divided into a clockwise polarized wave and a counterclockwise polarized wave. The two waves fluctuate at the frequencies of  $f_c - 2\alpha_0$  and  $f_c + 2\alpha_0$  respectively.

For the rotor of the outer rotor motor,  $f_c$  is 2226 Hz and  $\alpha_0$  is 46.38 rps (= 2783 rpm). Therefore, frequencies of the two polarized waves are calculated as following equation (3).

$$f_c - 2\alpha_0 \approx 2133 \text{ Hz}, \quad f_c + 2\alpha_0 \approx 2319 \text{ Hz} \quad (3)$$

These frequencies agree with the two peaks of noise shown in the Figure 11 and rotational directions also correspond to the results of the Figure 13 and 14 respectively. Therefore, the vibration displacements and the frequencies of measured electromagnetic noises are described with the formulas quantitatively.

Moving stationary wave                      Clockwise polarized wave                      Counterclockwise polarized wave

$$U(\theta, t) = U_0 e^{i2\theta} \frac{e^{i2\pi(f_c - 2\alpha_0)t} + e^{-i2\pi(f_c + 2\alpha_0)t}}{2}$$

$$U_{CW}(\theta, t) = \frac{U_0}{2} e^{i(2\theta + 2\pi(f_c - 2\alpha_0)t)}$$

$$U_{CCW}(\theta, t) = \frac{U_0}{2} e^{i(2\theta + 2\pi(f_c + 2\alpha_0)t)}$$

Figure 17 – Division of moving stationary wave into two polarized waves

## 5. CONCLUSIONS

It was clarified that resonating rotor with rotation causes electromagnetic noises with two different frequencies on an outer rotor motor.

Moreover, it was explained with formulas that the two frequencies are shifted positively or negatively by double the rotational speed from the resonance frequency in the case that the resonance mode shows ellipsoidal shape and the phenomenon was confirmed experimentally using non-stationary function of advanced conformal mapping by ESM approach.

## ACKNOWLEDGEMENTS

We would like to express our gratitude to staff members of Brüel & Kjær Sound & Vibration Measurement A/S, especially Mr. Jesper Gomes, for cooperating on developing non-stationary conformal mapping system and measuring electromagnetic noises.

## REFERENCES

1. Sun, Tao, et al. "Effect of pole and slot combination on noise and vibration in permanent magnet synchronous motor." *Magnetics*, IEEE Transactions on 47.5 (2011): 1038-1041.
2. Islam, Mohammad, Rakib Islam, and Tomy Sebastian. "Noise and vibration characteristics of permanent magnet synchronous motors using electromagnetic and structural analyses." *Energy Conversion Congress and Exposition (ECCE)*, 2011 IEEE. IEEE, 2011.
3. Islam, Rakib, and Iqbal Husain. "Analytical model for predicting noise and vibration in permanent-magnet synchronous motors." *Industry Applications*, IEEE Transactions on 46.6 (2010):



2346-2354.

4. Daisuke M, Itsuro K, and Naoki H. "Vibration Measurement for Rotating Disk Using Contactless Laser Excitation." Transactions of the Japan Society of Mechanical Engineers, Series C, Vol.77, No 784 (2011): 4402-4412.
5. Jesper G, Yutaka I, Bernard G. "Non-stationary Holography on Arbitrary Source Shapes." Proceedings of Internoise 2014.